

Cite this article as:

Boateng F, Ngwa W. Novel bioerodable eluting-spacers for radiotherapy applications with *in situ* dose painting. *Br J Radiol* 2019; **92**: 20180745.

FULL PAPER

Novel bioerodable eluting-spacers for radiotherapy applications with *in situ* dose painting

¹FRANCIS BOATENG, PhD and ^{2,3,4}WILFRED NGWA, PhD

¹Versant Medical Physics & Radiation Safety, MI, USA

²University of Massachusetts Lowell, Massachusetts, USA

³Brigham and Women's Hospital, Massachusetts, USA

⁴Harvard Medical School, Massachusetts, USA

Address correspondence to: Dr Francis Boateng

E-mail: Boatengfrancis09@gmail.com; Francis_Boateng@student.uml.edu

Objective: To investigate feasibility of using bioerodable/bioerodible spacers (BES) over biodegradable spacers (BDS) loaded with gold nanoparticles for radiotherapy applications with *in situ* dose-painting, and to explore dosimetric impact on dose enhancement ratio of different radioisotopes.

Methods: Analytical models proposed were based on experimentally reported erosion rate constant ($k_0 = 5.5E-7 \text{ kgm}^{-2}\text{s}^{-1}$) for bioerodible polymeric matrix. An *in vivo* determined diffusion coefficient ($2.2E-8 \text{ cm}^2/\text{s}$) of 10 nm gold nanoparticles (AuNP) of concentration 7 mg/g was used to estimate diffusion coefficient of other AuNP sizes (2, 5, 14 nm) using the Stoke-Einstein diffusion equation. The corresponding dose enhancement factors (DEF) were used to study dosimetric feasibility of employing AuNP-eluting BPS for radiotherapy applications.

Results: The results showed AuNP release period from BES was significantly shorter (116h) compared to BDS (more than a month) reported previously. The results also agree with reported Hopfenberg equation for a cylindrical matrix undergoing surface erosion. The DEF at tumour distance 5 mm for Cs-131 (DEF > 2.2) greater than that of I-125 (DEF > 2) and Pd-103 (DEF ≥ 2) could be achieved for AuNP sizes (2, 5, 10, and 14 nm) respectively.

Conclusion: Our findings suggested that BES could be used for short-lived radioisotopes like Pd-103 and Cs-131 in comparison to eluting BDS which is feasible for long-lived radioisotopes like I-125.

Advances in knowledge: The study provides scientific basis for development of new generation eluting spacers viable for enhancing localized tumour dose. It concludes that BES gives higher DEF for Cs-131, and good candidate for replacing conventional fiducials/spacers.

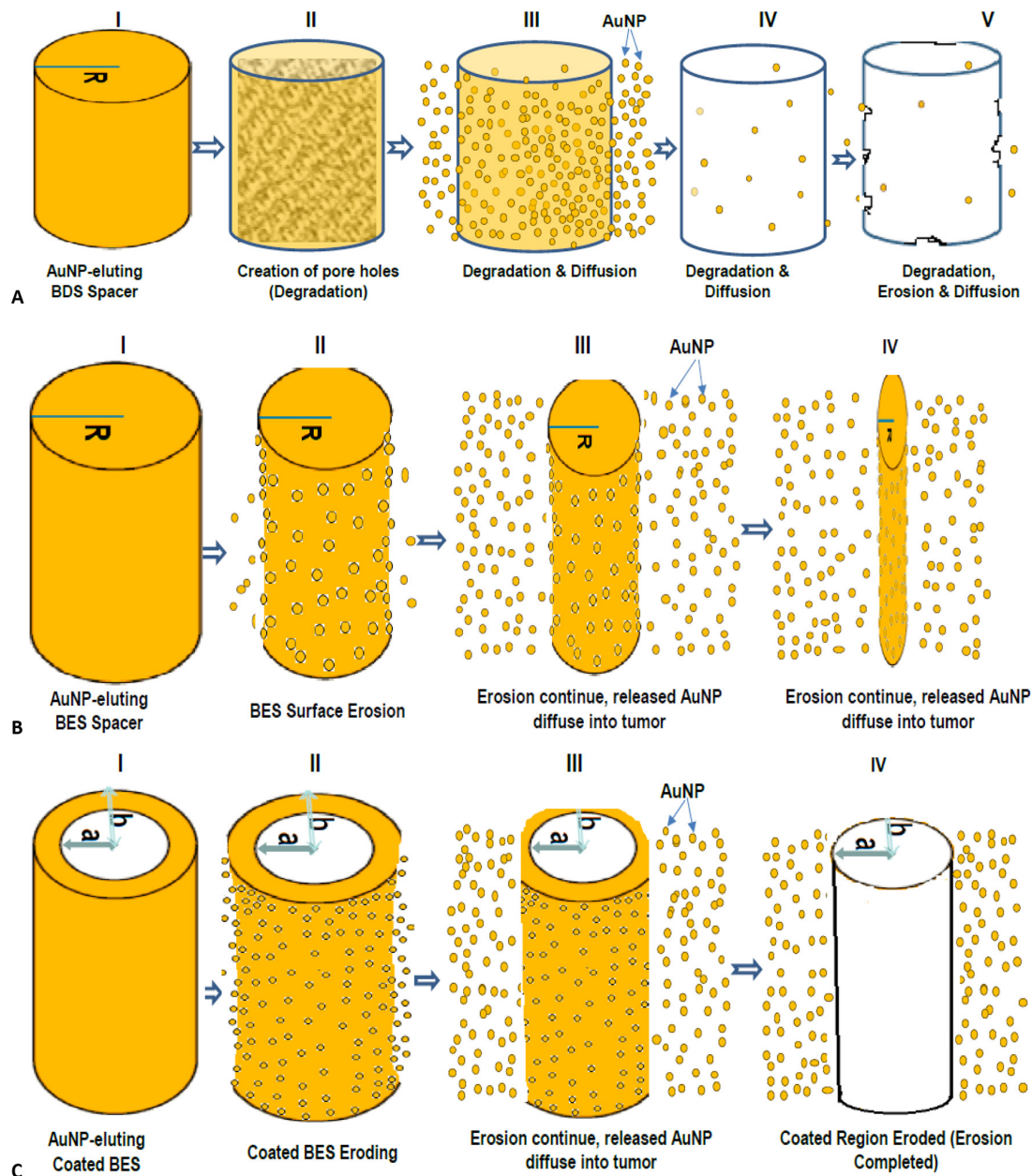
INTRODUCTION

Smart radiotherapy biomaterials (SRBs) loaded with radiosensitising [like gold nanoparticles (AuNP)] or anti-cancer drugs are being developed as viable multifunctional alternatives to conventional radiotherapy (RT) biomaterials (spacers, fiducials, beacons etc.) for RT applications.¹⁻⁹ The conventional inert RT biomaterials that are routinely used in RT have no direct radiotherapeutic contribution; however, they are essential for geometric accuracy to ensure reduction of dose toxicity to neighbouring healthy tissues.^{1-5,8,9} The proposed SRBs are new generation of fiducial markers or spacers loaded with anticancer agents or radiosensitisers like AuNP for *in situ* delivery (locally inside the tumour) for the purpose of increasing radiotherapeutic ratio without compromising their primary functions of the conventional RT biomaterials.^{1-5,8} Studies have shown that, after the administration of these SRBs, the AuNP/drug-loaded in the

SRBs are released inside the tumour subvolume, enhancing radiation dose during RT applications.^{1,3,4,10,11} However, the extent of dose enhancement depends on the amount of drug/nanoparticles (NP) released from the SRBs and diffused (drug/NP available) into the tumour cells to sensitise the cancerous cells before/during RT.¹ Since the rate of drug release from a matrix influences drug pharmacokinetics (movement of drug in the body/tumour resulting drug absorption, bioavailability, distribution, metabolism or excretion) which correlate to drug performance.¹²

The challenge is that the NP/drug release time can be extended from day(s) to weeks or months before sufficiently potent preload in the SRBs are released.^{1,5} For example, the experimental work of Nagesha et al showed that preload (Doxorubicin) release extended to over 3 months.⁵ As a result, the current reported studies suggested that only long-lived radioisotopes (like

Figure 1. Schematic diagram showing comparison between biodegradable and bioerodable/bioerodible polymeric AuNP-eluting spacers. (A) BDS (PLGA polymeric spacer degradation, as indicated in Boateng and Ngwa,¹ Figure 1D); (B) Erosion of BES loaded with AuNP; (C) Erosion of BES coated with AuNP. AuNP, gold nanoparticles; BES, bioerodible spacers; BDS, biodegradable spacers; PLGA, poly(d,l-lactic-co-glycolic acid).



iodine-125 (I-125) of half-life 59.4 days), would be good candidates for brachytherapy procedures due to the time it takes for the preload (NP/drug) to release from the SRBs.^{1,3} However, the rate of release of the preload (NP/drug) from the SRBs may depend on the complexities of the polymeric materials (like chitosan, poly(d,l-lactic-co-glycolic acid) (PLGA), etc.) used for fabrication of SRBs, and the fabrication method (compression, melt molding, spray-drying etc.).^{1,13-16} For instance, studies have shown that complex phenomena such as polymer degradation, erosion, swelling etc. influence preload release from polymeric implants like SRBs.^{1,13,14,17} In our previous study, we explored the effect PLGA degradation process on

preload release pattern from the spacers and recommended that preload release time should be accounted for during treatment planning.¹ SRBs made from biodegradable polymers (such as PLGA) are potential vehicle for loading anticancer chemotherapy agents or radiosensitisers, due to their high initial burst release rate in comparison to other biodegradable polymers.¹ However, the initial burst release might take days or week(s),^{1,18} which possess a challenge for the application of short-lived radioisotopes like Palladium-103 (Pd-103) of 17.0 days half-life and Cesium-131 (Cs-131) of half-life 9.7 days.¹ Since studies have shown Cs-131 seeds deliver a higher biological effective dose across a wide array of tumour types than

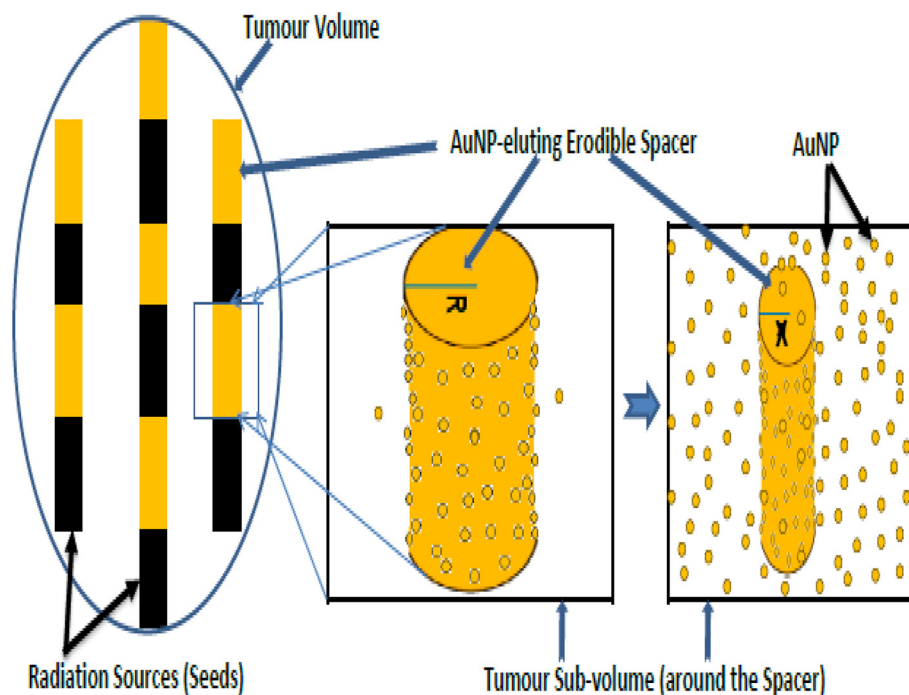
I-125 or Pd-103,¹⁹ it is appreciable to have eluting spacers that could release preload within hours or short period.

Nevertheless, other studies have shown that biologically eroding polymers (bioerodable^{20,21} or bioerodable^{22–25} polymers) such as polyanhydride have a great prospect for drug delivery in a short period (hours),^{23,26–28} and offer substantial drug delivery enhancements over orthodox delivery techniques.²⁷ Bioerodable/bioerodable polymers are polymers that undergo erosion phenomenon (surface or bulk) *in vivo* instead of degradation phenomenon (Figure 1) based on biological environmental conditions (either influenced by hydrolysis or microorganisms or both).^{16,29–31} Polymer erosion is the process of loss of material(s) from the polymer implant/matrix bulk.²⁹ This material loss may be oligomers, monomers, or portions of the polymer backbone or fragments of the polymer matrix bulk.²⁹ Bulk erosion is a homogeneous process in which polymer matrix erodes (inside-out) in a macroscopic scale,^{29,32–36} which involve the entire matrix.³³ That is bulk erosion result mass loss of material from the entire matrix,^{29,30,34,35} whereas, surface erosion is a heterogeneous process in which polymer matrix erodes (from outside to inward) in a microscopic scale.^{29,33,35} Thus, the polymer matrix/implant loses material in a small scale from the surface (exterior) only, keeping the original geometric shape (Figure 1B) while the implant get smaller and smaller until the whole implant erodes.^{16,17,30,33,34} The degree of bulk or surface erosion may drastically vary with the chemical structure of the polymer backbone.¹⁶ However, surface eroding polymers like polyanhydrides, poly(ortho esters), poly(desaminotyrosyl arylates),²¹ cellulose acetate phthalate and Pluronic F-127,²³ offer a constant drug release rate which is comparable (*i.e.* directly proportional) to polymer matrix erosion.^{23,32} Studies

have shown that drug release rate from these bioerodable polymers are reproducible and regulated,^{16,23,26} which would be suitable for designing SRBs for delivery of radiosensitizers like AuNP for dose enhancement during RT. Studies have also shown that polyanhydrides, for instance, are of great importance in drug delivery due to the fact that there is no reported evidence of inflammatory reaction, and they degrade well both *in vitro* and *in vivo* to acid byproducts as non-cytotoxic and non-mutagenic which does not need surgical removal after implantation from the tumour site.^{26,27,32,37} Implants such as Septacin (for local delivery of antibiotic to infected bone) and Gliadel (clinically used for treatment of brain cancer) which have been evaluated clinically are examples of implants made from polyanhydrides.^{26,28,38}

Herein, we explore the feasibility of using bioerodable or bioerodable polymers to fabricate SRB (*e.g.* spacer, see Figure 1B and C) loaded with gold nanoparticles (AuNP) for *in situ* dose painting, and to investigate dosimetric impact on dose enhancement ratio in RT applications (schematic diagram for prostate brachytherapy as an example is shown in Figure 2 below). In this study, surface bioerodable polymeric spacers (BES) were compared to biodegradable spacers (BDS) as we previously reported,¹ to provide scientific platform for fabrication of novel spacers for RT applications. Surface-eroding eluting spacers were evaluated as good candidates for brachytherapy application of short-lived radioisotopes like Pd-103 and Cs-131. Simplified models proposed for surface bioerodable spacers or implants based on experimental reported data were compared to Hopfenberg equation for a cylindrical matrix undergoing surface erosion.³⁹ This *in silico* study can also be useful to drug delivery field for guiding the design of surface erosion-controlled release implants.

Figure 2. Schematic diagram of AuNP-eluting erodible spacers for Brachytherapy Application (*e.g.*, Prostate tumour volume). AuNP, gold nanoparticles.



METHODS AND MATERIALS

Analytical models for surface eroding spacer were proposed based on the experimentally determined erosion rate constant ($k_0 = 5.5E-7 \text{ kgm}^{-2}\text{s}^{-1}$).^{40,41} Also, an *in vivo* pre-determined tumour diffusion coefficient D ($D = 2.2E-08 \text{ cm}^2/\text{s}$) for 10 nm AuNPs of concentration 7 mg/g,⁴² was used to determine diffusion coefficient of other AuNP sizes (2, 5, 14 nm), using the Stoke–Einstein diffusion equation^{1,3}. The dosimetric impact (dose enhancement ratio) of solid loaded bioerodable/bioerodible spacer was compared to conventional spacer coated with a mixture of bioerodible polymer and AuNP, as well as biodegradable spacer of the same dimensions, using different radioisotopes (e.g. I-125, Cs-131, and Pd-103) for brachytherapy applications. The spacer loaded with AuNP have dimensions of 2.0 mm diameter and length of 5.0 mm.^{4,43} The coated spacer has the same dimensions (but inner radius $a = 0.5 \text{ mm}$, outer radius $b = 1 \text{ mm}$, and length 5 mm like commercial spacers)⁴ as the solid loaded spacer. A Matlab R2015a software was used for calculations and plotting of the graphs. The schematic diagram of bioerodable/bioerodible spacer application in brachytherapy is shown Figure 2 below. The mathematical models derived are outlined below.

MODELLING BIOERODABLE SPACERS FOR RADIOTHERAPY APPLICATIONS

Considering a bioerodable or bioerodible cylindrical spacer (Figure 2 above) of radius R , length H , eroding at constant rate k_0 , loaded with AuNP/drug of initial concentration C_0 , uniformly distributed in the spacer (i.e. concentration $C = C_0$, for $x \leq r \leq R$, at time t), then the rate at which the spacer is eroding (change in radius) may be expressed as^{39,44},

$$\frac{dr}{dt} = -\frac{k_0}{C_0} \quad (1)$$

Integrating eqn. (1) with respect to the radius R and x resulted an expression given by^{39,44},

$$x = R - \frac{k_0 t}{C_0} = R \left(1 - \frac{k_0 t}{C_0 R} \right) \quad (2)$$

where R is initial radius of the spacer, x is the new radius of the eroded spacer (spacer remained as shown in Figure 2 above) at time t .^{39,44} Therefore, we provided a simplified approach for deriving the Hopfenberg equation,³⁹ for a cylindrical matrix undergoing surface erosion (the radius reducing inwardly). The amount of AuNP/drug released from the spacer into space–tumour interface at any time t , may be expressed as⁴⁵;

$$M_t = \pi R^2 H C_0 - 2\pi H \int_0^x C_0 r dr \quad (3)$$

Integrating eqn. (3), and substitute eqn. (2), we obtained;

$$M_t = \pi R^2 H C_0 - \pi H x^2 C_0 = \pi R^2 H C_0 \left[1 - \left(1 - \frac{k_0 t}{C_0 R} \right)^2 \right] \quad (4)$$

Since amount of AuNP/drug releasing from a cylindrical spacer/matrix at infinity (time, $t = \infty$) M_∞ , is given by⁴⁶;

$$M_\infty = \pi R^2 H C_0 \quad (5)$$

Substituting eqn. (5) into eqn. (4), we obtained Hopfenberg model for a cylindrical matrix undergoing erosion³⁹, expressed as;

$$\frac{M_t}{M_\infty} = 1 - \left(1 - \frac{k_0 t}{C_0 R} \right)^2 \quad (6)$$

where M_t and M_∞ is the amount of preload (AuNP/drug) released at time t , and at infinity (time, $t = \infty$) respectively. However, on average, the concentration profile of AuNP/drug releasing from the erodible cylindrical spacer may be expressed as⁴⁵;

$$C_R(t) = \frac{1}{\pi R^2 H} \int_0^{2\pi} \int_a^x \int_0^H r C_0 dz dr d\theta = \frac{2}{R^2} C_0 \int_R^x r dr = \frac{C_0}{R^2} [R^2 - x^2] \quad (7)$$

Substitute eqn. (2), into eqn. (7), we obtained;

$$C_R(t) = C_0 \left[1 - \left(1 - \frac{k_0 t}{C_0 R} \right)^2 \right] \quad (8)$$

where $C_R(t)$ is the concentration of AuNP/drug released from a cylindrical spacer eroding radially at time t , the meaning of other parameters remains the same. However, if erosion occur at both radial and laterally concurrently, then the rate at which the length of spacer is eroding ($L \leq z \leq H$, at time t , at constant rate k_z), may be expressed as;

$$\frac{dz}{dt} = -\frac{k_z}{C_0} \quad (9)$$

Integrating eqn. (9) with respect to the initial length H , and eroded length L , assuming the rate k_z is equal to k_0 , for simplicity. Then the resulted expression will be given by;

$$L = H - \frac{k_z t}{C_0} = H - \frac{k_0 t}{C_0} = H \left(1 - \frac{k_0 t}{C_0 H} \right) \quad (10)$$

where L is the length of eroding spacer remaining at time t . Subsequently, the total of amount of AuNP/drug released form cylindrical spacer eroding at time t , may be expressed as;

$$\begin{aligned} M_t &= \pi R^2 H C_0 - \int_0^{2\pi} \int_0^x \int_0^L r C_0 dz dr d\theta \\ &= \pi R^2 H C_0 - 2\pi L C_0 \int_0^x r dr = \pi R^2 H C_0 - \pi x^2 L C_0 \end{aligned} \quad (11)$$

Substituting eqn. (2), eqn. (6) and eqn. (10) into eqn. (11), we obtained;

$$\frac{M_t}{M_\infty} = 1 - \left(1 - \frac{k_0 t}{C_0 R} \right)^2 \left(1 - \frac{k_0 t}{C_0 H} \right) \quad (12)$$

The eqn. (12) is similar to expression obtained by Katzhendler et al for surface erosion via radial and axial directions.⁴⁴ Hence, the corresponding concentration profile $C_H(t)$, for a spacer eroding on both radial and lateral surfaces based on eqn. (11) & (12) is given by;

$$C_H(t) = C_0 \left[1 - \left(1 - \frac{k_0 t}{C_0 R} \right)^2 \left(1 - \frac{k_0 t}{C_0 H} \right) \right] \quad (13)$$

For a longer cylindrical spacer/matrix ($H \gg R$), as the length H approaches infinity, then eqn. (12) reduces to eqn. (6), and eqn. (13) becomes eqn. (8) respectively. Thus, for a long length, the erosion constant rate k_2 becomes insignificant.

MODELLING BIODEGRADABLE SPACERS FOR RADIOTHERAPY APPLICATIONS

A simplified model governing NP/drug release from the biodegradable polymeric spacer (e.g. PLGA spacer) as a result of both diffusion and polymer degradation kinetics due to initial burst release followed by a sustained release via diffusion process, was previously proposed, given by¹;

$$C_B(t) = C_0 * \left\{ F_I * [1 - \exp(-k_d t)] + F_D * \left[1 - \frac{4}{R^2} \sum_{n=1}^{\infty} \frac{1}{\alpha_n^2} \exp(-\alpha_n^2 D_0 t) \right] \right\} \quad (14)$$

where $C_B(t)$ is the total AuNP concentration released from eluting spacer to the spacer-tumour interface, C_0 is the initial AuNP concentration originally loaded in the spacer at time $t = 0$, k_d is first degradation rate constant for initial burst release ($k_d = 0.1076$ 1/day), F_I is the fraction of NP released as a result of initial burst, and F_D is the fraction of NP released via diffusion process; $F_I + F_D = 1$, R is the radius of a spacer (cylindrical) as shown in Figure 1, D_0 is the diffusion coefficient of the AuNPs released from the spacer,¹ and α_n ($\alpha_1 = 2.4048/R$, $\alpha_2 = 5.5201/R$, $\alpha_3 = 8.6537/R$, etc.) are roots ($J_0(x) = 0$) of Bessel function of first kind of zero order.^{1,45}

TUMOUR DRUG/AUNP DIFFUSION MODEL

From our previous study,¹ the AuNP/drug diffusing into the tumour cells may be expressed as¹;

$$C_T(x, t) = C_S(t) * \left[1 - \operatorname{erf}\left(\frac{x}{2\sqrt{D_T t}}\right) \right] \quad (15)$$

where x is the tumour distance, D_T is the diffusion coefficient of NP/drug in the tumour, $C(x, t)$ is the concentration of AuNP in the tumour cells at any time t , and $C_S(t)$ is the total concentration of GNP released from the spacer into the spacer-tumour interface via erosion-controlled release process $C_S(t)$ assumed to be zero ($C_S(t)=0$, at time $t = 0$), prior to diffusion of the preload into the tumour volume. However, the value of $C_S(t)$ at any time t , depends on the amount of AuNP released from the eroding spacer (radially, or both radial and lateral); i.e., $C_S(t)=C_R(t)$, $C_H(t)$, or $C_B(t)$ depending on equation (8), (13) or (14) respectively.

RESULTS

As illustrated in Figure 3 below, the study results show the release of AuNP from erodible spacers, based on well reported Hopfenberg equation (eqn. (6, see Figure 3a)) for a cylindrical matrix undergoing surface erosion,³⁹ which has been experimentally confirmed in the literature.^{26,44} Using erosion constant, $k_0 = 5.5E-7$ kgm⁻²s⁻¹ with spacer dimensions (radius, $R = 0.5$

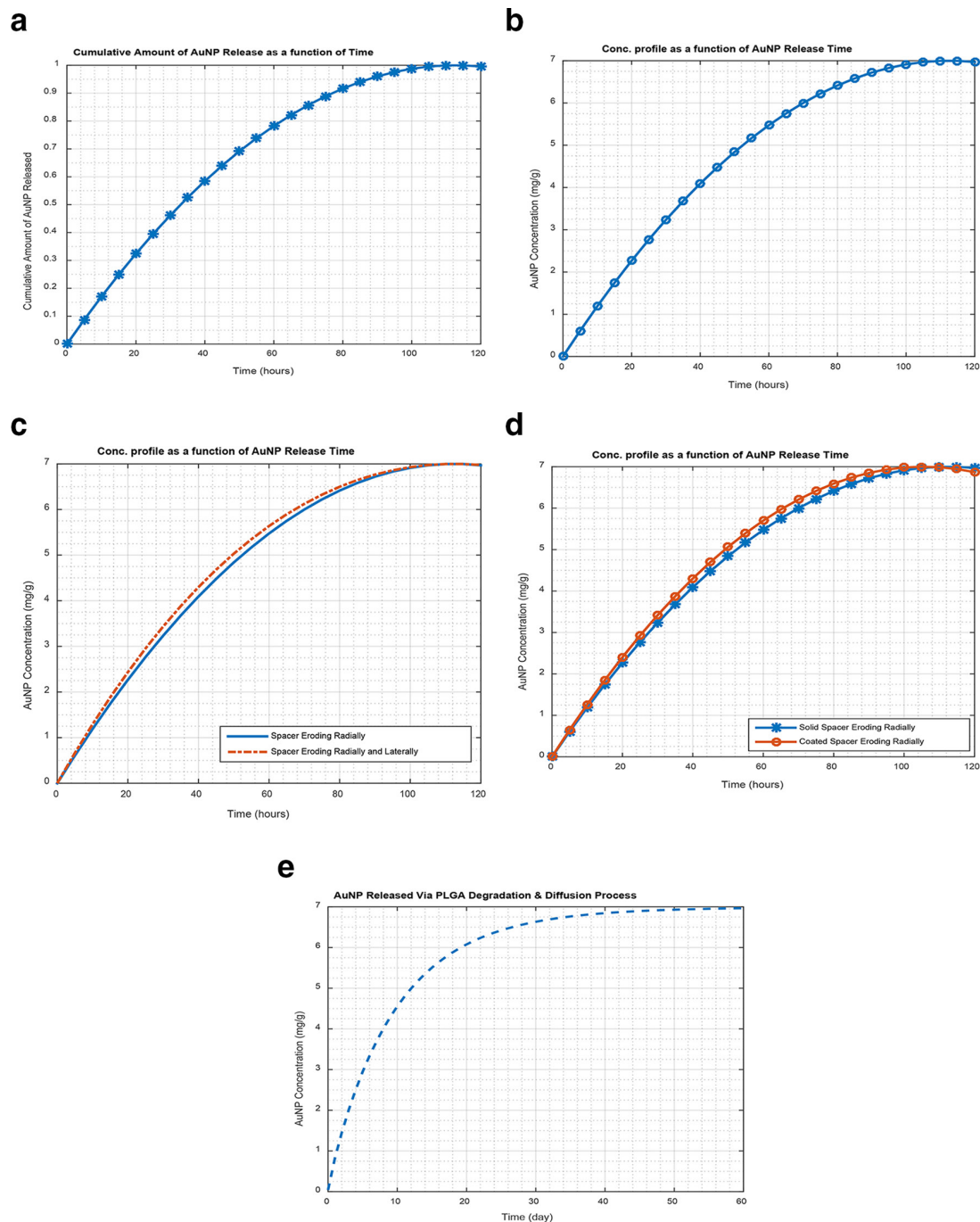
mm, length, $H = 5$ mm; volume = $2\pi R^2 H$) loaded with 10 nm AuNP of concentration 7 mg/g as an example. Figure 3a shows the cumulative fractional amount of AuNP released in hours (116 h \approx 5 days) based on Hopfenberg equation (eqn. (6)). The corresponding concentration profile (based on the proposed models, eqn. (8)) shown in Figure 3b, indicating the amount of GNP released in a specified period in comparison to its fractional amount released based on eqn. (6). Thus, Figure 3a and b show that the AuNP release period for bioerodable eluting spacers is shorter (hours) in comparison to the release period in over a month for biodegradable polymeric spacers reported in the literature.^{1,5} For instance, Figure 3e shows about 60 days release period for biodegradable space (using eqn. (14)), having the same dimensions as bioerodable spacer. However, Figure 3c shows comparison between spacers eroding radially (eqn. (8)), and spacers eroding both radially and laterally (eqn. (13)). The solid-line in Figure 3c shows surface erosion occurring radially using eqn. (8), whereas the dash-line indicates surface erosion occurring both radially and laterally (along the length) using eqn. (13) respectively. Figure 3c also, shows that for a longer release time, the eqn. (13) becomes equal to eqn. (8), but differ for a short period. However, Figure 3d shows comparison between commercial spacer coated with a mixture of erodible polymer and AuNP (Coated erodible spacer, see Figure 1c), and spacers made from a mixture of erodible polymer and AuNP (Solid loaded erodible spacer, Figure 1b). Figure 3d shows that for two erodible spacers (coated (Figure 1c), and solid spacers (Figure 1b)) with the same dimensions. The coated spacers have potential of releasing content quicker (about 100 h) than the solid loaded spacer (116 h), due to the difference in diameters. Thus, coated erodible spacer have inert inner radius equal to the radius (0.5 mm) of the conventional commercial spacer with no AuNP confined within. The AuNP in the coated spacers are confined within a smaller radius in comparison to the solid spacer. Therefore, assuming the same constant erosion rate, the coated spacers was expected to release its content/preload faster than solid spacer as shown Figure 3d.

However, Figure 4 below demonstrates, the dose enhancement factor (DEF; the ratio of dose with AuNP to dose without AuNP) as a function of time at a tumour distance 5 mm from an erodible spacer loaded with different AuNP sizes (2, 5, 10, and 14 nm) of tumour diffusion coefficient of 11×10^{-8} , 4.4×10^{-8} , 2.2×10^{-8} , and 1.5×10^{-8} cm²/s respectively; which were determined from the diffusion coefficient of the 10 nm AuNP using Stoke-Einstein diffusion equation^{1,3}. It can be seen in Figure 4 that Cs-131 has a higher DEF (>2.2) than I-125 (DEF >2) and Pd-103 have DEF ≥ 2 for all AuNP sizes (2-, 5-, 10-, and 14 nm) considered in this study as illustrated below.

DISCUSSION

The results shown in Figure 3 above, demonstrated that bioerodable/bioerodable smart spacers can release preload (AuNP/drug) in a short period (in hours or few days) in accordance with Hopfenberg equation for cylindrical erodible matrix (eqn. (6)). This can be useful for delivering anticancer drugs or radiosensitisers to enhance RT efficacy, especially for short-lived brachytherapy seeds/radioisotopes (e.g. Cs-131 or Pd-103). The results also

Figure 3. A release profile for 10 nm AuNP (concentration 7 mg/g) released from eluting-spacer; (a) Cumulative Amount of AuNP released using Hopfenberg equation (eqn. (6)), (b) Concentration profile for a solid erodible spacer using eqn. (8), (c) Concentration Profile for solid erodible spacer loaded with AuNP using eqn. (8) & (13), (d) Concentration profile comparing coated erodible spacer to solid erodible spacer with AuNP using eqn. (8), (e) Concentration profile of biodegradable spacer loaded with AuNP, using eqn. (14). AuNP, gold nanoparticles.



confirm the experimental results reported that erodible polymers like Polyanhydrides are appropriate for short-term delivery of bioactive agents.^{26,44} Thus, *in vivo* and *in vitro* release characteristics of a wide-range of drug and proteins like insulin, growth factors, enzymes etc. imbedded in Polyanhydrides implants have been reported.¹⁶ For instance, drug (amoxicillin) released from hydroxypropyl methylcellulose tablets were described as a

controlled release exclusively by erosion of the tablets,⁴⁴ which occurred in hours depending on the tablets sizes. Therefore, our study results suggest that it is feasible to use drug/NP-loaded erodible brachytherapy spacers for brachytherapy applications for both short and long-lived radioisotopes depending on the design in comparison to degradable spacers which is feasible for only long-lived radioisotopes as we reported previously.¹ Thus,

Figure 4. DEF as a function of time at a distance of 5 mm from erodible spacer eluting AuNP of different sizes with AuNP concentration of 7 mg/g; a) Cs-131 source (seed), (b) I-125 source, (c) Pd-103 source. AuNP, gold nanoparticles; DEF, dose enhancement factor.

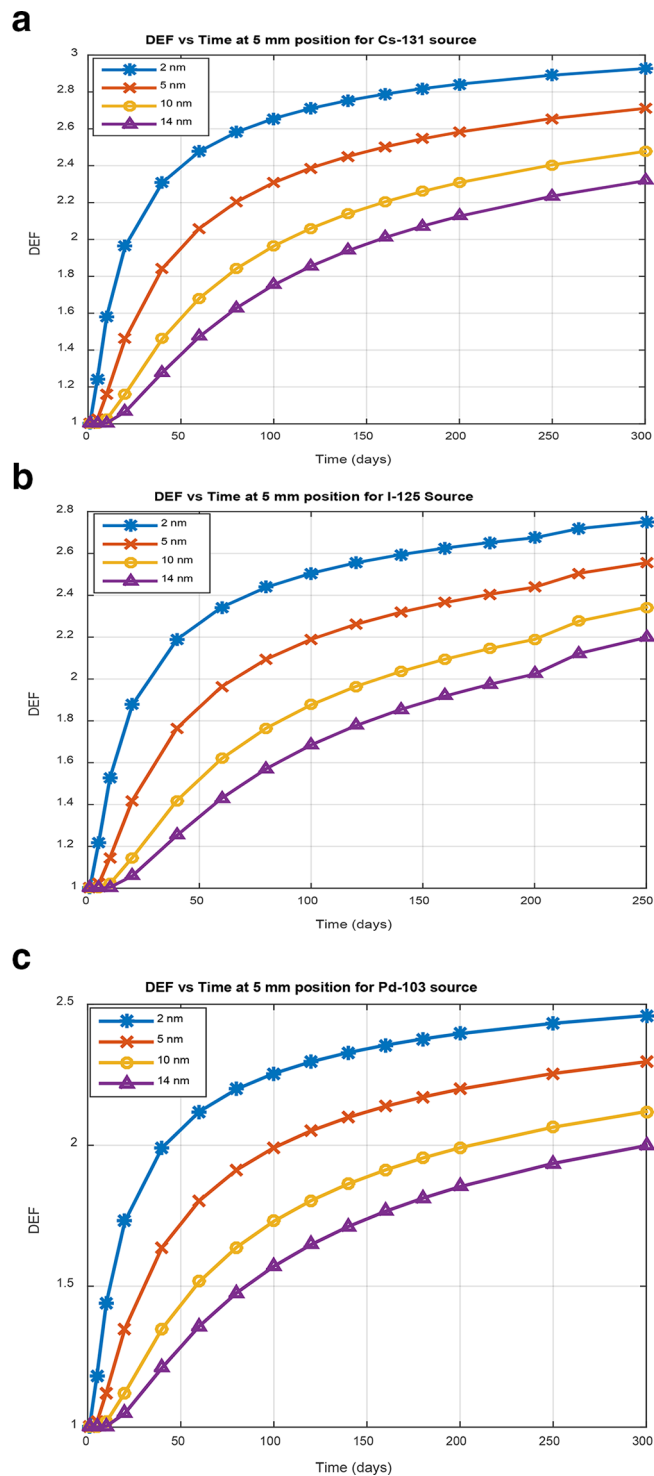


Figure 4 shows dosimetric feasibility of using erodible spacer for both short- and long-lived radioisotopes due to the short AuNP release time from the erodible spacers. Since Cs-131 has a higher DEF than that of I-125, it is advisable to employ erodible smart

spacers for brachytherapy application with *in situ* dose painting. Other studies have shown that in 33 days, Cs-131 delivers about 90% of the prescribed dose to the tumour compared to 32% for I-125.⁴⁷ Making it significant to employ smart spacers to enhance the delivery dose within short period, eliminating the possibility of recurrence or sublethal radiation dose delivery to tumour.

However, surface erosion process was preferred over bulk erosion in this study due to the reported short drug release time from surface-eroding polymers in comparison to bulk-eroding polymers (like poly(ester), poly(d,l-lactic acid), poly(glycolic acid), poly(ϵ -caprolactone), polyamide, proteins, and cellulose (and its derivatives)).^{16,17,29,31,35} Thus, bulk erosion takes a long time without eroding until the polymer matrix spontaneously erode (erupt inside-out), with mass loss of material from the bulk matrix, making it unclear how to determine the polymers matrix erosion in one way or the other.^{31,35} Studies also have shown that surface eroding matrices are mostly appropriate for sustained release and for drug preservation.²⁷ It should be emphasized that, the surface erosion phenomenon displayed by bioerodable polymeric implants can be modulated by tailoring the implant/spacer to produce controlled release profiles of preloads which are predictable, and that can vary from hours to days, weeks or months, dependent on the chemistry of the polymer used.^{27,37} Thus, the zero-order release kinetics exhibited by erodible polymers could be prolonged from week to a month, for sustained release of preload (NP/drug) by combining erodible polymers (*e.g.* polyanhydrides) with different erosion rates to obtain the desired results.^{27,44} For instance, studies show that drug release rate from implants made from polyanhydride could be altered over a thousand times by varying the polymer backbone.³² The extent of surface erosion can be altered by changing the surface area of the matrix or reducing water uptake by using polymers with hydrophobic monomer units, or by adding hydrophobic excipients to stabilize the matrix erosion rate.¹⁶ Though, the erosion rates of erodible polymers can be controlled by varying composition of polymers (as the hydrophobicity of monomer increases, the anhydride bond becomes more stable to hydrolysis), the degree of erosion depends on the polymer type. For example, aliphatic polyanhydrides erode within days while aromatic polyanhydrides erosion can be extended to many years.¹⁶

However, polymer erosion process contends with other mechanisms like diffusion for dominion. When erosion is faster than other processes like diffusion, then drug release becomes erosion-controlled.³⁰ Since polymer erosion is a very complex phenomenon, other processes such as dissolution, swelling, degradation, and diffusion of oligomers and monomers, as well as morphological changes of the polymeric matrix may occur concurrently during polymer erosion.^{33,37,48} Drug delivery via erosion controlled-release processes allow drug release to be predictable, but when other process(es) is/are considered, it is difficult to take into account all the processes in erosion controlled released quantitatively.³⁰ Besides, drug release rate agrees with complete polymer matrix erosion which is suitable for polymer biocompatibility, and biodistribution.³⁰

Nevertheless, the mathematical models provided can precisely predict release profile of preload incorporated in surface erodible

spacers and matrices for drug/NP delivery, since these models are comparable to Hopfenberg equation for a cylindrical matrix undergoing surface erosion,³⁰ which have been confirmed by experimental results.^{23,44} This implies, the models can be useful for drug delivery fields, and can be used to predict the release profiles of one or multilayered drug-loaded matrices. For instance, the cumulative drug release model for radial surface erosion (eqn. (6), with a corresponding concentration model, eqn. (8)), and the model both radial and lateral erosion (eqn. (12), with corresponding concentration model, eqn. (13)) have been successfully verified experimentally for erodible tablets by Katzhendler et al.⁴⁴ Therefore, drug-loaded spacers/fiducial markers proposed for biological *in situ* dose painting, to enhance therapeutic efficiency during image-guided radiation treatments,⁵ can be replaced with erodible spacers that undergo both radial and lateral erosion with reference to eqn. (13). It should be noted that, the diffusion model (eqn. (15)) do not account for tumour environment, which might affect the rate of diffusion of the released AuNPs into the tumour. Our future studies will be focused on AuNP tumour diffusion and the subsequent effect on concentration with respect to different tumour types.

The purpose of this study was practically to provide a platform that guides experimental approach for designing suitable surface-eroding spacers loaded with radiosensitizing anticancer agents

for *in situ* delivery of the agents during RT applications. Also, to encourage other researchers to independently investigate (*in vivo* and *in vitro*) the feasibility of using surface erodible polymers (e.g. polyanhydrides, poly(ortho esters), etc.) and their copolymers appropriate for RT applications. Successful development of such technologies can lead to clinical trials, replacing currently used inert RT biomaterials with erodible SRBs. The erodible spacers can be designed to release preload (drug/nanoparticles) from hours to days, weeks or months for specific applications in RT, and a good replacement for the conventional inert spacers or fiducials.

CONCLUSION

The results highlighted therapeutic advantage of bioerodable/bioerodible smart spacers over biodegradable spacers, in that the preload release period from erodible smart spacer was shorter (116 h). The results correlate with the experimental results of drug release from erodible matrices in hours reported in the literature. The findings suggest that erodible AuNP-eluting spacers can be employed for short-lived radioisotopes like Pd-103 and Cs-131 as well as long-lived radioisotopes like I-125 in comparison to biodegradable eluting spacers feasible for only long-lived radioisotopes. The results also highlighted the therapeutic advantage of Cs-131 which offers highest dose enhancement than I-125, and Pd-103 respectively.

REFERENCES

1. Boateng F, Ngwa W. Modeling gold nanoparticle-eluting spacer degradation during brachytherapy application with *in situ* dose painting. *Br J Radiol* 2017; **90**: 20170069: 20170069. doi: <https://doi.org/10.1259/bjr.20170069>
2. Ngwa W, Boateng F, Kumar R, Irvine JD, Formenti S, Ngoma T, et al. Smart radiotherapy biomaterials. *Int J Radiat Oncol Biol Phys* 2017; **2017**: 624–37.
3. Sinha N, Cifter G, Sajo E, Kumar R, Sridhar S, Nguyen PL, et al. Brachytherapy application with *in situ* dose painting administered by gold nanoparticle eluters. *Int J Radiat Oncol Biol Phys* 2015; **91**: 385–92. doi: <https://doi.org/10.1016/j.ijrobp.2014.10.001>
4. Cormack RA, Sridhar S, Suh WW, D'Amico AV, Makrigiorgos GM. Biological *in situ* dose painting for image-guided radiation therapy using drug-loaded implantable devices. *Int J Radiat Oncol Biol Phys* 2010; **76**: 615–23. doi: <https://doi.org/10.1016/j.ijrobp.2009.06.039>
5. Nagesha DK, Tada DB, Stambaugh CKK, Gultepe E, Jost E, Levy CO, et al. Radiosensitizer-eluting nanocoatings on gold fiducials for biological *in-situ* image-guided radio therapy (BIS-IGRT). *Phys Med Biol* 2010; **55**: 6039–52. doi: <https://doi.org/10.1088/0031-9155/55/20/001>
6. Altundal Y, Cifter G, Detappe A, Sajo E, Tsiamas P, Zygmanski P, et al. New potential for enhancing concomitant chemoradiotherapy with FDA approved concentrations of cisplatin via the photoelectric effect. *Phys Med* 2015; **31**: 25–30. doi: <https://doi.org/10.1016/j.ejmp.2014.11.004>
7. Cifter G, Altundal Y, Detappe A, Sajo E, Berbeco R, Makrigiorgos Met al. Dose enhancement during concomitant chemoradiotherapy using FDA approved concentrations of carboplatin and oxaliplatin nanoparticles. In: Jaffray D, ed. *World Congress on Medical Physics and Biomedical Engineering, June 7-12, 2015, Toronto, Canada. IFMBE Proceedings. vol 51*. Springer: Cham; 2015. pp. 1723–6.
8. Kumar R, Belz J, Markovic S, Jadhav T, Fowle W, Niedre M, et al. Nanoparticle-based brachytherapy spacers for delivery of localized combined chemoradiation therapy. *Int J Radiat Oncol Biol Phys* 2015; **91**: 393–400. doi: <https://doi.org/10.1016/j.ijrobp.2014.10.041>
9. Boateng F. *In silico* study of smart radiotherapy biomaterials for radiotherapy applications. *University of Massachusetts Lowell, ProQuest Dissertations Publishing* 2017; **10675302**: 1–118.
10. Ngwa W, Makrigiorgos GM, Berbeco RI. Gold nanoparticle-aided brachytherapy with vascular dose painting: estimation of dose enhancement to the tumor endothelial cell nucleus. *Med Phys* 2012; **39**: 392–8. doi: <https://doi.org/10.1118/1.3671905>
11. Ngwa W, Makrigiorgos GM, Berbeco RI. Applying gold nanoparticles as tumor-vascular disrupting agents during brachytherapy: estimation of endothelial dose enhancement. *Phys Med Biol* 2010; **55**: 6533–48. doi: <https://doi.org/10.1088/0031-9155/55/21/013>
12. Gopferich A, Langer R. Modeling of polymer erosion. *Macromolecules* 1993; **26**: 4105–12. doi: <https://doi.org/10.1021/ma00068a006>
13. Alexis F, Venkatraman SS, Rath SK, Boey F. *In vitro* study of release mechanisms of paclitaxel and rapamycin from drug-incorporated biodegradable stent matrices. *J Control Release* 2004; **98**: 67–74. doi: <https://doi.org/10.1016/j.jconrel.2004.04.011>
14. Charlier A, Leclerc B, Couarraze G. Release of mifepristone from biodegradable matrices: experimental and theoretical evaluations. *Int J Pharm* 2000; **200**: 115–20. doi: [https://doi.org/10.1016/S0378-5173\(00\)00356-2](https://doi.org/10.1016/S0378-5173(00)00356-2)
15. Blanco MD, Sastre RL, Teijón C, Olmo R, Teijón JM. Degradation behaviour of microspheres prepared by spray-drying poly(D,L-lactide) and poly(D,L-lactide-

- co-glycolide) polymers. *Int J Pharm* 2006; **326**(1-2): 139–47. doi: <https://doi.org/10.1016/j.ijpharm.2006.07.030>
16. Uhrich KE, Cannizzaro SM, Langer RS, Shakesheff KM. Polymeric systems for controlled drug release. *Chem Rev* 1999; **99**: 3181–98. doi: <https://doi.org/10.1021/cr940351u>
 17. Chen Y, Zhou S, Li Q. Mathematical modeling of degradation for bulk-erosive polymers: applications in tissue engineering scaffolds and drug delivery systems. *Acta Biomater* 2011; **7**: 1140–9. doi: <https://doi.org/10.1016/j.actbio.2010.09.038>
 18. Engineer C, Parikh J, Raval A. Hydrolytic degradation behavior of 50-50 poly lactide-co-glycolide from drug. *Trends Biomater Artif Organs* 2010; **24**: 131–8.
 19. Armpilia CI, Dale RG, Coles IP, Jones B, Antipas V. The determination of radiobiologically optimized half-lives for radionuclides used in permanent brachytherapy implants. *Int J Radiat Oncol Biol Phys* 2003; **55**: 378–85. doi: [https://doi.org/10.1016/S0360-3016\(02\)04208-6](https://doi.org/10.1016/S0360-3016(02)04208-6)
 20. Mathiowitz E, Jacob JS, Jong YS, Carino GP, Chickering DE, Chaturvedi P, et al. Biologically erodable microspheres as potential oral drug delivery systems. *Nature* 1997; **386**: 410–4. doi: <https://doi.org/10.1038/386410a0>
 21. Jaffe M, Pai V, Ophir Z, Wu J, Kohn J. Process-structure-property relationships of erodable polymeric biomaterials, I: Poly(desaminotyrosyl arylates. *Polym Adv Technol* 2002; **13**(10-12): 926–37. doi: <https://doi.org/10.1002/pat.278>
 22. Rosen HB, Chang J, Wnek GE, Linhardt RJ, Langer R. Bioerodible polyanhydrides for controlled drug delivery. *Biomaterials* 1983; **4**: 131–3. doi: [https://doi.org/10.1016/0142-9612\(83\)90054-6](https://doi.org/10.1016/0142-9612(83)90054-6)
 23. Sundararaj SC, Thomas MV, Dziubla TD, Puleo DA. Bioerodible system for sequential release of multiple drugs. *Acta Biomater* 2014; **10**: 115–25. doi: <https://doi.org/10.1016/j.actbio.2013.09.031>
 24. Zuleger S, Lippold BC. Polymer particle erosion controlling drug release. I. Factors influencing drug release and characterization of the release mechanism. *Int J Pharm* 2001; **217**(1-2): 139–52. doi: [https://doi.org/10.1016/S0378-5173\(01\)00596-8](https://doi.org/10.1016/S0378-5173(01)00596-8)
 25. Einmahl S, Behar-Cohen F, Tabatabay C, Savoldelli M, D'Hermies F, Chauvaud D, et al. A viscous bioerodible poly(ortho ester) as a new biomaterial for intraocular application. *J Biomed Mater Res* 2000; **50**: 566–73. doi: [https://doi.org/10.1002/\(SICI\)1097-4636\(20000615\)50:4<566::AID-JBM12>3.0.CO;2-M](https://doi.org/10.1002/(SICI)1097-4636(20000615)50:4<566::AID-JBM12>3.0.CO;2-M)
 26. Kumar N, Langer RS, Domb AJ. Polyanhydrides: an overview. *Adv Drug Deliv Rev* 2002; **54**: 889–910. doi: [https://doi.org/10.1016/S0169-409X\(02\)00050-9](https://doi.org/10.1016/S0169-409X(02)00050-9)
 27. Kipper MJ, Shen E, Determan A, Narasimhan B. Design of an injectable system based on bioerodible polyanhydride microspheres for sustained drug delivery. *Biomaterials* 2002; **23**: 4405–12. doi: [https://doi.org/10.1016/S0142-9612\(02\)00181-3](https://doi.org/10.1016/S0142-9612(02)00181-3)
 28. Li LC, Deng J, Stephens D. Polyanhydride implant for antibiotic delivery--from the bench to the clinic. *Adv Drug Deliv Rev* 2002; **54**: 963–86. doi: [https://doi.org/10.1016/S0169-409X\(02\)00053-4](https://doi.org/10.1016/S0169-409X(02)00053-4)
 29. Siepmann J, Göpferich A. Mathematical modeling of bioerodible, polymeric drug delivery systems. *Adv Drug Deliv Rev* 2001; **48**(2-3): 229–47. doi: [https://doi.org/10.1016/S0169-409X\(01\)00116-8](https://doi.org/10.1016/S0169-409X(01)00116-8)
 30. Göpferich A. Erosion of composite polymer matrices. *Biomaterials* 1997; **18**: 397–403. doi: [https://doi.org/10.1016/S0142-9612\(96\)00151-2](https://doi.org/10.1016/S0142-9612(96)00151-2)
 31. von Burkersroda F, Schedl L, Göpferich A. Why degradable polymers undergo surface erosion or bulk erosion. *Biomaterials* 2002; **23**: 4221–31.
 32. Jain JP, Modi S, Domb AJ, Kumar N. Role of polyanhydrides as localized drug carriers. *J Control Release* 2005; **103**: 541–63. doi: <https://doi.org/10.1016/j.jconrel.2004.12.021>
 33. Göpferich A. Mechanisms of polymer degradation and erosion. *Biomaterials* 1996; **17**: 103–14. doi: [https://doi.org/10.1016/0142-9612\(96\)85755-3](https://doi.org/10.1016/0142-9612(96)85755-3)
 34. Lyu S, Untereker D. Degradability of polymers for implantable biomedical devices. *Int J Mol Sci* 2009; **10**: 4033–65. doi: <https://doi.org/10.3390/ijms10094033>
 35. Lyu S, Sparer R, Untereker D. Analytical solutions to mathematical models of the surface and bulk erosion of solid polymers. *J Polym Sci B Polym Phys* 2005; **43**: 383–97. doi: <https://doi.org/10.1002/polb.20340>
 36. Fu Y, Kao WJ. Drug release kinetics and transport mechanisms of non-degradable and degradable polymeric delivery systems. *Expert Opin Drug Deliv* 2010; **7**: 429–44. doi: <https://doi.org/10.1517/17425241003602259>
 37. Torres MP, Vogel BM, Narasimhan B, Mallapragada SK. Synthesis and characterization of novel polyanhydrides with tailored erosion mechanisms. *J Biomed Mater Res A* 2006; **76A**: 102–10. doi: <https://doi.org/10.1002/jbm.a.30510>
 38. Jain JP, Chitkara D, Kumar N. Polyanhydrides as localized drug delivery carrier: an update. *Expert Opin Drug Deliv* 2008; **5**: 889–907. doi: <https://doi.org/10.1517/17425247.5.8.889>
 39. Hopfenberg HB. Controlled release from Erodible slabs, cylinders, and spheres. *Controlled Release Polymeric Form* 1976; **33**: 26–32.
 40. Chirico S, Dalmoro A, Lamberti G, Russo G, Titomanlio G. Analysis and modeling of swelling and erosion behavior for pure HPMC tablet. *J Control Release* 2007; **122**: 181–8. doi: <https://doi.org/10.1016/j.jconrel.2007.07.001>
 41. Siepmann J, Kranz H, Bodmeier R, Peppas NA. HPMC-matrices for controlled drug delivery: a new model combining diffusion, swelling, and dissolution mechanisms and predicting the release kinetics. *Pharm Res* 1999; **16**: 1748–56. doi: <https://doi.org/10.1023/A:1018914301328>
 42. Wong C, Stylianopoulos T, Cui J, Martin J, Chauhan VP, Jiang W, et al. Multistage nanoparticle delivery system for deep penetration into tumor tissue. *Proceedings of the National Academy of Sciences* 2011; **108**: 2426–31. doi: <https://doi.org/10.1073/pnas.1018382108>
 43. Shirato H, Harada T, Harabayashi T, Hida K, Endo H, Kitamura K, et al. Feasibility of insertion/implantation of 2.0-mm-diameter gold internal fiducial markers for precise setup and real-time tumor tracking in radiotherapy. *Int J Radiat Oncol Biol Phys* 2003; **56**: 240–7. doi: [https://doi.org/10.1016/S0360-3016\(03\)00076-2](https://doi.org/10.1016/S0360-3016(03)00076-2)
 44. Katzhendler I, Hoffman A, Goldberger A, Friedman M. Modeling of drug release from erodible tablets. *J Pharm Sci* 1997; **86**: 110–5. doi: <https://doi.org/10.1021/js9600538>
 45. Barrer RM. *Diffusion in and through solids*. New York, NY: The University Press; 1941.
 46. Fu JC, Hagemer C, Moyer DL. A unified mathematical model for diffusion from drug-polymer composite tablets. *J Biomed Mater Res* 1976; **10**: 743–58. doi: <https://doi.org/10.1002/jbm.820100507>
 47. Wernicke AG, Yondorf MZ, Peng L, Trichter S, Nedialkova L, Sabbas A, et al. Phase I/II study of resection and intraoperative cesium-131 radioisotope brachytherapy in patients with newly diagnosed brain metastases. *J Neurosurg* 2014; **121**: 338–48. doi: <https://doi.org/10.3171/2014.3.JNS131140>
 48. Göpferich A, Tessmar J. Polyanhydride degradation and erosion. *Adv Drug Deliv Rev* 2002; **54**: 911–31. doi: [https://doi.org/10.1016/S0169-409X\(02\)00051-0](https://doi.org/10.1016/S0169-409X(02)00051-0)